Hydroclimatic variations in southeastern China during the 4.2 ka event reflected by stalagmite records

Haiwei Zhang[1,2], Hai Cheng[1,3], Yanjun Cai[2,1], Christoph Spötl[4], Gayatri Kathayat[1], Ashish Sinha[5],
R. Lawrence Edwards[3], and Liangcheng Tan[2,1,6]

[1]Institute of Global Environmental Change, Xi'an Jiaotong University, Xi'an 710054, China

[2]Institute of Earth Environment, Chinese Academy of Sciences, State Key Laboratory of Loess and Quaternary Geology, Xi'an 710061, China

[3]Department of Earth Sciences, University of Minnesota, Minneapolis, Minnesota 55455, USA

[4]Institute of Geology, University of Innsbruck, Innsbruck 6020, Austria

[5]Department of Earth Science, California State University Dominguez Hills, Carson, California 90747, USA

[6]Open Studio for Oceanic-Continental Climate and Environment Changes, Pilot National Laboratory for Marine Science and Technology (Qingdao), Qingdao 266061, China

Corresponding to: Haiwei Zhang (zhanghaiwei@xjtu.edu.cn)

Abstract. The collapses of several Neolithic cultures in China are considered to have been associated with abrupt climate change during the 4.2 ka event (4.2-3.9 ka BP). The hydroclimate of this event in southeastern China, however, is still poorly known, except for a few published records from the lower reaches of Yangtze River. In this study, a high-resolution record of monsoon precipitation between 5.3 and 3.6 ka BP based on a stalagmite from Shennong cave, Jiangxi Province, southeast China, is presented. Coherent variations in δ^{18}O and δ^{13}C reveal that the climate in this part of China was dominantly wet between 5.3 and 4.5 ka BP and mostly dry between 4.5 and 3.6 ka BP, interrupted by a wet interval (4.3-4.05 ka BP). A comparison with other records from monsoonal China suggests that monsoon precipitation decreased in northern China but increased in southern China during the 4.2 ka event. We propose that the weakened East Asian summer monsoon controlled by the reduced Atlantic Meridional Overturning Circulation resulted in this contrasting distribution of monsoon precipitation between north and south China. During the 4.2 ka event the rain belt remained longer at its southern position, giving rise to a pronounced humidity gradient between northern and southern China.

1 Introduction

The 4.2 ka event was a pronounced climate event in the Holocene which has been widely

studied in the past 20 years. It was identified as an abrupt (mega)drought and/or cooling event in a variety of natural archives including ice cores, speleothems, lake sediments, marine sediments, and loess. This climate episode was associated with the collapse of several ancient civilizations and human migrations in many sites worldwide (e.g., Egypt, Greece, the Indus Valley and the

40   Yangtze Valley) (Weiss et al., 1993; Cullen et al., 2000; Gasse, 2000; DeMenocal, 2001; Weiss and Bradley, 2001; Thompson et al., 2002; Booth et al., 2005; Bar-Matthews and Ayalon, 2011; Berkelhammer et al., 2012; Ruan et al., 2016). Recently, the 4.2 ka event was defined as the lower boundary of the Meghalayan Stage by the International Commission on Quaternary Stratigraphy. The chronology of this geological boundary is defined at a specific level in a stalagmite from

45   northeast India (http://www.stratigraphy.org/).

    The climate change associated with the 4.2 ka event also significantly affected ancient civilizations in China, resulting in the collapses of Neolithic cultures (Jin and Liu, 2002; Huang et al., 2010, 2011; Wu et al., 2017). Most of these studies imply a temperature drop in continental China at about 4.2 ka BP (Yao and Thompson, 1992; Jin and Liu, 2002; Zhou et al., 2002; Xu et

50   al., 2006; Yao et al., 2017; Zhao et al., 2017), but changes in the spatial distribution of precipitation are also discussed (Tan et al., 2008; Huang et al., 2010, 2011; Tan et al., 2018a, 2018b; Wu et al., 2017). For example, a grain-size record from Daihai Lake, north China, suggests a decrease in monsoon precipitation between 4.4 and 3.1 ka BP with a very dry interval between 4.4 and 4.2 ka BP (Peng et al., 2005). Extreme flooding during the 4.2 ka event was identified by

55   paleoflood deposits in the middle reaches of the Yellow River (Huang et al., 2010, 2011). Wu et al. (2017) reported evidence of two extraordinary paleoflood events in the middle reaches of the Yangtze River at 4.9-4.6 ka BP and 4.1-3.8 ka BP, closely related to the expansion of the Jianghan lakes. These extreme hydroclimate events may have accelerated the collapse of the Shijiahe Culture in the middle reaches of the Yangtze River (Wu et al., 2017). Multiple proxies in four

60   stalagmites from Xianglong cave, south of the Qinling Mountains, indicate that the upper Hanjiang River region experienced a wet climate during the 4.2 ka event (Tan et al., 2018a). Peat records provide a broad picture of climate variations in southeast China (SEC) during the Holocene (Zhou et al., 2004; Zhong et al., 2010a, 2010b, 2010c, 2015, 2017). The resolution of these records, however, is not high enough to study the detailed structure of the 4.2 ka event. Until

65   now, there is only one published stalagmite record from SEC (Xiangshui cave; Fig. 1), indicating a wet interval during the 4.2 ka event (Zhang et al., 2004).

    The aim of this study was to obtain a high-resolution stalagmite-based record from SEC to explore the hydroclimatic variations during the 4.2 ka event and to compare them to records in northern China in order to explore the possible north-south precipitation gradient during this

70   event.

2 Study area and sample

Shennong Cave (117°15' N, 28°42' E, 383 m a.s.l.) is located in the northeast of Jiangxi Province, SEC (Fig. 1), a region in the mid-subtropical zone that is strongly influenced by the East Asian summer monsoon (EASM). Mean annual precipitation and temperature at the nearest meteorological station (Guixi; 1951-2010 AD) are 1857 mm and 18.5 °C, respectively (Fig. 2a). The rainy season includes both summertime monsoon rainfall and spring persistent rain (Tian and Yasunari, 1998; Wan et al., 2008; Zhang et al., 2018). The latter is a unique synoptic and climatic phenomenon that occurs from March until mid-May, mostly south of the Yangtze River (about 24°N to 30°N, 110°E to 120°E - Tian and Yasunari, 1998; Wan and Wu, 2007, 2009). EASM precipitation lasts from mid-May to September (Wang and Lin, 2002). Shennong cave is located in the region of the spring persistent rain. Data from the nearest GNIP station in Changsha, also located in the region of the spring persistent rain, indicate that the EASM (May to September) precipitation with lower $\delta^{18}O$ values (Figs. 2a, b) accounts for 54% of the annual precipitation and the non-summer monsoon (NSM) (October to next April) precipitation with higher $\delta^{18}O$ values (Figs. 2a, b) accounts for 46% (Zhang et al., 2018).

The cave was discovered by local people in 1998 after several days of continuous heavy rain. The cave developed in Carboniferous limestone of the Chuan-shan and Huang-long Groups, which are mainly composed of limestone and interbedded dolostone. The thickness of the cave roof ranges from about 20 to about 80 m, with an average of ~50 m. The overlying vegetation consists mainly of secondary forest tree species such as *Pinus*, *Taxodiaceae* and bamboo and shrub-like *Camelliaoleifera* and *Ilex bioritsensis* which are C_3 plants (Zhang et al., 2015). According to two years' monitoring (2011-2013), the mean temperature in the cave is 19.1 °C with a standard deviation of 2.5 °C (Fig. 2c), consistent with mean annual air temperature outside the cave (Fig. 2a). The relative humidity in the interior of the cave approaches 100% during the most of the year (Fig. 2c). Abundant aragonite and calcite speleothems are present in the cave. Their mineralogy is likely controlled by the Mg/Ca ratio of the drip water reflecting the variable dolomite content of the limestone (De Choudens-Sanchez and Gonzalez, 2009; Zhang et al., 2014, 2015). All aragonite stalagmites were deposited within ~1.5 km of the cave entrance where the bedrock is dolomite and all calcite stalagmites were deposited in more distal parts of the cave where limestone constitutes the bedrock.

In November 2009 stalagmite SN17 (Fig. 3), 320 mm in length, was collected 200 m behind the cave entrance where the bedrock is dolomite. X-ray diffraction (XRD) analyses suggest that the stalagmite is composed of aragonite, except for the bottom section below 318 mm which is composed of calcite (Fig. 3). The calcite section was not included in the present study.

3 Methods

3.1 ^{230}Th dating

Eleven subsamples for ^{230}Th dating were drilled along the growth axis of SN17 (Fig. 3) with

110   a hand-held carbide dental drill, and were dated on a multi-collector inductively coupled plasma

mass spectrometer (MC-ICP-MS, Neptune-Plus) at the Department of Earth Sciences, University

of Minnesota and the Institute of Global Environmental Change, Xi'an Jiaotong University

(Cheng et al., 2000, 2013). The chemical procedure used to separate uranium and thorium

followed those described by Edwards et al. (1987).

115

3.2 Stable isotope analyses

120 sub-samples for stable isotope analyses were drilled along the central axis of SN17 at

intervals of 1 mm between 0 and 70 mm and 5 mm between 70 and 320 mm distance from top,

respectively. The samples were analysed using a gas-source stable isotope ratio mass spectrometer

120   (Isoprime100), equipped with a MultiPrep system at the Institute of Earth Environment, Chinese

Academy of Sciences (IEECAS). The international standard NBS19 and the laboratory standard

HN were analysed after every 10 sub-samples to monitor data reproducibility. All oxygen and

carbon isotope compositions are reported in per mil relative to the Vienna Pee Dee Belemnite

(VPDB). Reproducibility of δ^{18}O and δ^{13}C values was better than 0.1‰ and 0.08‰ (2σ),

125   respectively.

4 Results

4.1 Chronology

The ^{230}Th dates are all in stratigraphic order and no hiatus was observed (Table 1). Because

130   of the high uranium concentrations (1120-6380 ppb) and relative low thorium concentrations

(56-195 ppt), most of the dating errors are less than 6‰. We used a linear interpolation method to

establish a depth-age model of stalagmite SN17 which grew from 3643 to 5299 a BP (Fig. 3).

4.2 δ^{13}C and δ^{18}O records

135   The temporal resolution of the δ^{13}C and δ^{18}O records ranges from 6 to 21 years. The δ^{13}C

values fluctuate around -9.18‰ (mean value) during the period 5.3 to 4.5 ka BP, and increase to

-8.69‰ between 4.5 and 3.6 ka BP (Fig. 4a). δ^{18}O fluctuates around -6.75‰ (mean value) during

the period 5.3 to 3.6 ka BP, without a significant long-term trend (Fig. 4c). The δ^{18}O record is

broadly similar to the δ^{13}C record between 5.3 and 3.6 ka BP, with a significantly positive

140   correlation (Fig. 5a, r=0.29, p<0.01). δ^{18}O and δ^{13}C values show a statistically significant

covariance along the growth axis suggesting that the speleothem was not deposited under isotopic equilibrium (Hendy, 1971; Dorale and Liu, 2009). Several studies, however, demonstrated that stalagmites showing a significant correlation between $\delta^{18}O$ and $\delta^{13}C$ can also have formed under isotopic equilibrium, indicating they are controlled by the common influencing factors (Dorale et

145 al., 1998; Dorale and Liu, 2009; Tan et al., 2018a). Another, more robust test is the replication of $\delta^{18}O$ records from different caves (Dorale et al., 1998; Wang et al., 2001; Dorale and Liu, 2009; Cai et al., 2010). The $\delta^{18}O$ records of SN17 and of stalagmites from Dongge (Wang et al., 2005) and Xiangshui (Zhang et al., 2004) caves, located southwest of Shennong cave (Fig. 1), show remarkable similarities during the overlapping interval (Fig. 6). The replication of these records

150 further confirms that aragonite of stalagmite SN17 was most likely deposited close to isotopic equilibrium, i.e., the $\delta^{18}O$ variation primarily reflects climatic changes. The growth rate of SN17 shows a persistently decreasing trend from 0.62 to 0.034 mm/yr between 5.2 and 4.5 ka BP, followed by low values during the period 4.5 to 3.6 ka BP with relatively higher values between 4.25 and 4.0 ka BP (Fig. 4e).

155

4 Discussion

4.1 Interpretation of $\delta^{18}O$ and $\delta^{13}C$

The climatic significance of the $\delta^{18}O$ parameter in speleothems from the monsoon region of China has been intensively debated in recent years, because it is influenced by several, partly

160 competing factors including precipitation amount, moisture source and transport pathway, upstream depletion and changes in the ratio of the amount of summer to winter precipitation, as well as the cave temperature (Maher, 2008; Clemens et al., 2010; Dayem et al., 2010; Pausata et al., 2011; Caley et al., 2014; Tan, 2014). Most scientists agree that speleothem $\delta^{18}O$ values in monsoonal China represent variations in the EASM intensity and/or changes in

165 spatially-integrated precipitation between different moisture sources and the cave site on orbital to millennial timescales rather than local precipitation amount (Cheng et al., 2016). Some researchers suggest that the speleothem $\delta^{18}O$ value in south China is not influenced by precipitation amount or EASM intensity but by moisture circulation on interannual to interdecadal (He et al., 2009; Tan, 2009, 2014) or even on centennial to millennial timescales (Tan, 2016). According to the specific

170 seasonal distribution of precipitation amount and $\delta^{18}O$ values in the region of spring persistent rain, we suggest that the speleothem $\delta^{18}O$ from E'mei cave, located at 160 km northwest of Shennong cave, is primarily controlled by the ratio of EASM precipitation amount to NSM precipitation amount (EASM/NSM) on interannual timescales (Zhang et al., 2018). In addition, the speleothem $\delta^{18}O$ record from E'mei cave also shows a significant correlation with the EASM precipitation

175 amount during 1951-2009 AD, and exhibits a coherent variation with the drought/flood index on

interannual to centennial timescales for the interval 1810-2000 AD (Zhang et al., 2018). This indicates that the speleothem δ^{18}O values in Shennong cave, similar to that in E'mei cave, can be also influenced by the EASM precipitation amount on interannual to centennial timescales.

Speleothem δ^{13}C is influenced by many processes from the soil via the vadose zone to cave

180 environment (Genty et al., 2003; McDermott, 2004; Fairchild et al., 2006 and references therein). Many studies suggest that changes in speleothem δ^{13}C are generally controlled by vegetation density and composition in the catchment which vary according to the hydroclimate (Genty et al., 2001, 2006; Baldini et al., 2005; Cruz Jr et al., 2006; Fleitmann et al., 2009). Soil CO_2, which is produced by root respiration and organic matter decomposition, dissolved in the drip water drives

185 speleothem δ^{13}C. In regions where the vegetation type is predominantly C_3 or C_4 plants, a dry climate will lead to a reduction of the vegetation cover, density and soil microbial activity as well as an increase in the groundwater residence time allowing more δ^{13}C-enriched bedrock to be dissolved. In addition, Prior calcite precipitation (PCP) in the vadose zone will result in higher δ^{13}C values accompanied by increased Mg/Ca ratios in speleothems (Baker et al., 1997). Slow drip

190 rates and increased evaporation and/or ventilation inside the cave will lead to higher δ^{13}C values, usually accompanied by kinetic isotopic fractionation (Fairchild et al., 2000; Frisia et al., 2011; Li et al., 2011; Tremaine et al., 2011).

In Jiangxi Province, a region presently occupied by mostly C_3 plants, no evidence has been found for a general pattern of replacement of C_3 plants by C_4 plants during the late Holocene

195 (Zhou et al., 2004; Zhong et al., 2010b). There is no significant positive correlation between δ^{13}C values and Mg/Ca ratios between 5.3 and 3.6 ka BP (Fig. 5b). In Shennong cave ventilation is weak and relative humidity remains close to 100% throughout the year. Rapid CO_2 degassing is inhibited under these conditions. Stalagmite SN17 was likely deposited close to isotopic equilibrium, as confirmed by the replication test (section 4.2). The δ^{13}C variations in this

200 stalagmite were therefore not controlled by PCP or rapid CO_2 degassing. Rather, changes in δ^{13}C were driven by vegetation density and soil bioproductivity associated with hydroclimatic variations, with lower δ^{13}C values corresponding to a dense vegetation cover associated with a wet climate and vice versa (Zhang et al., 2015).

205 **4.2 Hydroclimate between 5.3 and 3.6 ka BP**

Previous speleothem studies from monsoonal China suggested a coherent trend of decreasing precipitation from the early to the late Holocene (Dykoski et al., 2005; Wang et al., 2005; Hu et al., 2008; Cai et al., 2010, 2012; Dong et al., 2010, 2015; Jiang et al., 2013; Bai et al., 2017; Tan et al., 2018a), which follows the gradually decreasing Northern Hemisphere summer insolation. Our

210 δ^{13}C record exhibits a similarly increasing trend (Figs. 4a, b), indicating that the climate in our

study area changed from wet to dry condition between 5.3 and 3.6 ka BP. The long-term trend in $\delta^{18}O$ is less significant than $\delta^{13}C$ (Figs. 4c, d) and might be caused by changes in seasonality of the precipitation amount and $\delta^{18}O$ (see section 2). Because speleothem $\delta^{18}O$ values reflect the amount-weighted annual precipitation $\delta^{18}O$ value, in our study area, the EASM precipitation with lower $\delta^{18}O$ values accounts for 54% of the annual precipitation and the NSM precipitation with higher $\delta^{18}O$ values (Figs. 2a, b) accounts for 46% (Zhang et al., 2018). Therefore, we found that speleothem $\delta^{18}O$ in our study area are significantly influenced by the changes in the EASM/NSM ratio on interannual timescales (Zhang et al., 2018). A decreasing intensity of EASM might lead to changes in the EASM/NSM ratio and in turn result in variations in speleothem $\delta^{18}O$, however, it remains unclear how the EASM and NSM precipitation amount varied on centennial to millennial timescale, respectively. Therefore, the long-term trend in $\delta^{18}O$ is less significant than that in $\delta^{13}C$. But we still find that there were more wet intervals (z-scored $\delta^{18}O$ values > 0) between 5.3 and 4.5 ka BP than between 4.5 and 3.6 ka BP on centennial timescales (Fig. 4d). The $\delta^{18}O$ record shows similar variations as the $\delta^{13}C$ record (Figs. 4b, d), which are not related to seasonal variations of $\delta^{18}O$ values in precipitation on centennial to millennial timescales. In addition, the SN17 $\delta^{18}O$ record is remarkably similar to the $\delta^{18}O$ record from Dongge cave (Fig. 6), which is primarily controlled by summer monsoon precipitation (Dykoski et al., 2005; Wang et al., 2005). These observations indicate that variations in SN17 $\delta^{18}O$ might reflect changes in summer monsoon precipitation on decadal to millennial timescales, with higher (lower) $\delta^{18}O$ values representing decreased (increased) summer monsoon precipitation. The conspicuously decreasing trend in growth rate further confirms that the monsoon precipitation gradually decreased from 5.3 to 3.6 ka BP (Fig. 4e). During 4.5-3.6 ka BP, a wet interval between 4.3 and 4.05 ka BP can be identified in our $\delta^{18}O$ record (Fig. 4d) on centennial timescales, consistent with high values of growth rate between 4.25 and 4.0 ka BP. The low values of $\delta^{13}C$ record between 4.15 and 3.95 ka BP (Fig. 4b), however, lags the decreased $\delta^{18}O$ record by 150 years. The asynchronously decreased variations between the $\delta^{13}C$ and $\delta^{18}O$ may be ascribed to the delayed response of enhanced vegetation density to increased monsoon precipitation. Two decadal intervals with decreased $\delta^{18}O$ values during the period 3.95 to 3.8 ka BP cannot be found in the $\delta^{13}C$ record and the growth rate of SN17 (Fig. 4), indicating they are two insignificantly wet events. Therefore, we suggest that the climate in our study area between 5.3 and 4.5 ka BP was dominantly wet, and changed to a rather dry climate between 4.5 and 3.6 ka BP with one wet interval between 4.3 and 4.05 ka BP (Fig. 4). Our $\delta^{18}O$ and $\delta^{13}C$ records exhibit a two-stage structure during the 4.2 ka event, characterized by a wet phase with high variability between 4.3 and 4.05 ka BP and a distinctly dry phase from 4.05 to 3.6 ka BP.

A record of total organic carbon (TOC) from Dahu swamp, Jiangxi Province, located 450 km

south of Shennong cave, indicates a dry climate between 6.0 and 4.0 ka BP, with an short-lived wet event at 4.1 ka BP (Zhou et al., 2004). Subsequent multi-proxy records of several new cores from this site also revealed a prevailingly dry climate between 6.0 and 3.0 ka BP with a wet interval at 4.2-3.9 ka BP (Zhong et al., 2010a, 2010b, 2010c) Speleothem $\delta^{18}O$ record from

250   Xiangshui cave also exhibits a remarkable similarity to the SN17 $\delta^{18}O$ record, showing a wet interval between 4.2 and 4.0 ka BP (Fig. 6). These published records from SEC are consistent with our isotope records within error, indicating a wet climate in SEC during 4.2 ka event.

4.3 Comparison with other records in monsoonal China covering the 4.2 ka event

255   The remarkable drought during 4.2 ka event was recorded by various archives from different sites in northern and southwestern China (Tan et al., 2008; 2018; Zhao et al., 2010; Chen et al., 2015; Goldsmith et al., 2017 and references therein). In contrast, the extraordinary flood during the 4.2 ka event was identified in the middle reaches of the Yellow River in north-central China (Huang et al., 2010, 2011) and the middle reaches of the Yangtze River in south-central China

260   (Wu et al., 2017). For SEC, $\delta^{15}N$ and $\delta^{13}C$ records from the Daping swamp (Fig. 1) reveal a wet interval of 4.5-4.0 ka BP (Zhong et al., 2017), however, other proxies from the same site indicate cool and dry climate between 4.5 and 3.5 ka BP (Zhong et al., 2015). Pollen data of two sediment profiles from the Daiyunshan Mountain (Fig. 1), SEC, indicate a centennial-scale wet event at 4.4 ka BP (Zhao et al., 2017). A dry and cold period during 4.2 ka event was identified in a sediment

265   profile near Taihu Lake (Fig. 1), East China (Yao et al., 2017). To sum up, records from lacustrine, peat and paleoflood sediments suggest that the climate during the 4.2 ka event was dry in northern and southwestern China and wet in central and southern China (Fig. 8), although there are discrepancies in some records from southern China, which might be caused by the large dating uncertainties and the low resolution. Tan et al. (2018) has already proposed the same "north-dry

270   and south-wet" pattern by reviewing records from the monsoon region of China; however, more speleothem records from SEC are needed to further confirm this pattern.

         In the following discussion only high-precision and high-resolution speleothem records are used. Two stalagmite $\delta^{18}O$ records from Nuanhe and Lianhuadong caves in northern China indicate that the climate between 4.0 and 3.5 ka BP was very dry (Tan and Cai, 2005; Dong et al.,

275   2015). Another two stalagmite $\delta^{18}O$ records from Jiuxian and Xianglong caves south of the Qinling Mountains revealed increased monsoon precipitation in central China during the 4.2 ka event (Fig. 7a, b; Cai et al., 2010; Tan et al., 2018a). Stalagmite $\delta^{18}O$ records from Sanbao (Fig. 7c; Dong et al., 2010), Heshang (Fig. 7d; Hu et al., 2008) and Lianhua (Zhang et al., 2013) caves in the middle reaches of Yangtze River, south-central China, also indicate a wet interval between

280   4.15 and 3.9 ka BP, which is consistent with a $\delta^{13}C$ record of peat from the Dajiuhu basin (Figs. 7e;

Ma et al., 2008) in the same region. The SN17 δ^{18}O record also reveals a wet interval between 4.3 and 4.05 ka BP on centennial timescales (Fig. 7g). These records reveal a coherently dry period in northern China but a wet climate in south-central and southeastern China during 4.2 ka event (Fig. 7).

285   This south-north distribution of monsoon precipitation might have been caused by weakened EASM intensity, which could have resulted from a reduced Atlantic Meridional Overturning Circulation (AMOC) recorded by higher amounts of ice-rafted debris (IRD) in the North Atlantic (Figs. 7g-i). Strong freshwater input into the North Atlantic derived from melting icebergs periodically reduced the AMOC (Bond et al., 2001), causing a southward migration of the

290 Intertropical Convergence Zone and a weakened EASM (Wang et al., 2001). During these intervals, the rain belt migrated southward and remained longer at this position, which reduced rainfall in northern China but enhanced rainfall in central and southern China (Tan et al., 2011, 2018a; Zhang et al., 2014; Chiang et al., 2015).

    The SN17 δ^{18}O record exhibits a coherent variation with the δ^{18}O record from Dongge cave

295 within error, showing four wet intervals between 4.6 and 3.8 ka BP on centennial timescales (Figs. 7f, g). These four wet intervals were also identified in other stalagmite δ^{18}O records, although there are some differences in the amplitude (Fig. 7). For example, the first wet interval in the SN17 δ^{18}O record corresponds to the dry interval in the δ^{18}O records from Jiuxian and Xianglong caves. A reason for this discrepancy might be chronology offsets, because these records are

300 constrained by two dates only. Alternatively, monsoon precipitation in our study area during this period was out of phase with those in the region around Jiuxian and Xianglong caves. Because at 4.55 ka BP the AMOC was in a very weak stage, this could have resulted in a weakened EASM and a further southward shift of the monsoonal rain belt, possibly causing a dry climate in south-central China and a wet climate in SEC. The different amplitudes of the other three wet

305 intervals in these speleothem records from central to southern China might have been caused by the spatial distribution of monsoon precipitation, reflecting the position and residence time of the rain belt associated with variations in EASM intensity.

5 Conclusions

310 We reconstructed monsoon precipitation variations in the lower Yangtze River region, SEC, between 5.3 and 3.6 ka BP based on δ^{18}O and δ^{13}C records of a precisely dated, high-resolution stalagmite from Shennong cave in the northern part of Jiangxi Province. The long-term trend of increasing δ^{18}O and δ^{13}C values together a decreasing growth rate is consistent with other stalagmite and peat records from monsoonal China, showing increased monsoon rainfall between

315 5.3 and 4.5 ka BP and decreased monsoon rainfall between 4.5 and 3.6 ka BP in the study area. A

wet episode at 4.3-4.05 ka BP in our record is in agreement with other records from southern China. A dry climate in northern China and a coeval wet climate in southern China during the 4.2 ka event may have been caused by a weakened summer monsoon, which itself may have been related to a reduced Atlantic Meridional Overturning Circulation. During a weak summer

320 monsoon, the rain belt remains longer in its southern position, resulting in reduced precipitation in northern China and enhanced precipitation in southern China. Four wet intervals between 4.6 and 3.8 ka BP were identified in our δ^{18}O record and agree within dating error with other stalagmite δ^{18}O records from monsoonal China. Small discrepancies in the individual δ^{18}O records during these four intervals may reflect chronology offsets or a spatial distribution of monsoon

325 precipitation associated with variations in summer monsoon intensity.

6 Author Contributions

H.W.Z. designed the research and wrote the first draft of the manuscript. H.C. Y.J.C. C.S. and A.S. revised the manuscript. H.W.Z. and Y.J.C. did the field work and collected the samples. H.W.Z.

330 Y.J.C. and L.C.T. conducted the oxygen isotope measurements. H.W.Z. H.C. G.K. and R.L.E. conducted the ^{230}Th dating. All authors discussed the results and provided input on the manuscript.

7 Competing interests

The authors declare no competing financial interests.

335

8 Acknowledgments

This study was supported by the NSFC (41502166), NSFC (41731174), NSFC (41731174), the China Postdoctoral Science Foundation (2015M580832), the Key Laboratory of Karst Dynamics, Ministry of Land and Resources of the People's Republic of China (MLR) and GZAR
340 (KDL201502), the State Key Laboratory of Loess and Quaternary Geology (SKLLQG1046), and the Shaanxi Science Fund for Distinguished Young Scholars (2018JC-023)

9 References

Bai, Y., Zhang, P., Gao, T., Yu, R., Zhou, P., and Cheng, H.: The 5400 a BP extreme weakening
345   event of the Asian summer monsoon and cultural evolution, Science China Earth Sciences,
            2017. 1-12, 2017.
Baker, A., Ito, E., Smart, P. L., and McEwan, R. F.: Elevated and variable values of 13C in
            speleothems in a British cave system, Chemical Geology, 136, 263-270, 1997.
Baldini, J., McDermott, F., Baker, A., Baldini, L., Mattey, D., and Railsback, L. B.: Biomass
350   effects on stalagmite growth and isotope ratios: A 20th century analogue from Wiltshire,
            England, Earth and Planetary Science Letters, 240, 486-494, 2005.
Bar-Matthews, M. and Ayalon, A.: Mid-Holocene climate variations revealed by high-resolution
            speleothem records from Soreq Cave, Israel and their correlation with cultural changes, The

Holocene, 21, 163-171, 2011.

355   Berkelhammer, M., Sinha, A., Stott, L., Cheng, H., Pausata, F. S., and Yoshimura, K.: An abrupt
        shift in the Indian monsoon 4000 years ago, Geophys. Monogr. Ser, 198, 2012.

Booth, R. K., Jackson, S. T., Forman, S. L., Kutzbach, J. E., Bettis Iii, E., Kreigs, J., and Wright, D.
        K.: A severe centennial-scale drought in midcontinental North America 4200 years ago and
        apparent global linkages, The Holocene, 15, 321-328, 2005.

360   Cai, Y., Tan, L., Cheng, H., An, Z., Edwards, R. L., Kelly, M. J., Kong, X., and Wang, X.: The
        variation of summer monsoon precipitation in central China since the last deglaciation, Earth
        and Planetary Science Letters, 291, 21-31, 2010.

Cai, Y., Zhang, H., Cheng, H., An, Z., Edwards, R. L., Wang, X., Tan, L., Liang, F., Wang, J., and
        Kelly, M.: The Holocene Indian monsoon variability over the southern Tibetan Plateau and its
365   teleconnections, Earth and Planetary Science Letters, 335, 135-144, 2012.

Caley, T., Roche, D. M., and Renssen, H.: Orbital Asian summer monsoon dynamics revealed
        using an isotope-enabled global climate model, Nature communications, 5, 5371, 2014.

Chen, F., Xu, Q., Chen, J., Birks, H. J. B., Liu, J., Zhang, S., Jin, L., An, C., Telford, R. J., and Cao,
        X.: East Asian summer monsoon precipitation variability since the last deglaciation,
370   Scientific reports, 5, 11186, 2015.

Cheng, H., Edwards, R. L., Shen, C.-C., Polyak, V. J., Asmerom, Y., Woodhead, J., Hellstrom, J.,
        Wang, Y., Kong, X., and Spötl, C.: Improvements in ^{230}Th dating, ^{230}Th and ^{234}U half-life
        values, and U–Th isotopic measurements by multi-collector inductively coupled plasma mass
        spectrometry, Earth and Planetary Science Letters, 371, 82-91, 2013.

375   Cheng, H., Edwards, R. L., Sinha, A., Spötl, C., Yi, L., Chen, S., Kelly, M., Kathayat, G., Wang,
        X., Li, X., Kong, X., Wang, Y., Ning, Y., and Zhang, H.: The Asian monsoon over the past
        640,000 years and ice age terminations, Nature, 534, 640-646, 2016.

Cheng, H., Edwards, R., Hoff, J., Gallup, C., Richards, D., and Asmerom, Y.: The half-lives of
        uranium-234 and thorium-230, Chemical Geology, 169, 17-33, 2000.

380   Clemens, S. C., Prell, W. L., and Sun, Y.: Orbital-scale timing and mechanisms driving Late
        Pleistocene Indo-Asian summer monsoons: Reinterpreting cave speleothem δ^{18}O,
        Paleoceanography, 25, PA4207, 2010.

Cruz Jr, F. W., Burns, S. J., Karmann, I., Sharp, W. D., Vuille, M., and Ferrari, J. A.: A stalagmite
        record of changes in atmospheric circulation and soil processes in the Brazilian subtropics
385   during the Late Pleistocene, Quaternary Science Reviews, 25, 2749-2761, 2006.

Cullen, H. M., deMenocal, P. B., Hemming, S., Hemming, G., Brown, F. H., Guilderson, T., and
        Sirocko, F.: Climate change and the collapse of the Akkadian empire: Evidence from the deep
        sea, Geology, 28, 379-382, 2000.

Dayem, K. E., Molnar, P., Battisti, D. S., and Roe, G. H.: Lessons learned from oxygen isotopes in
390   modern precipitation applied to interpretation of speleothem records of paleoclimate from
        eastern Asia, Earth and Planetary Science Letters, 295, 219-230, 2010.

De Choudens-Sanchez, V. and Gonzalez, L. A.: Calcite and aragonite precipitation under
        controlled instantaneous supersaturation: elucidating the role of CaCO$_3$ saturation state and
        Mg/Ca ratio on calcium carbonate polymorphism, Journal of Sedimentary Research, 79,
395   363-376, 2009.

DeMenocal, P. B.: Cultural responses to climate change during the late Holocene, Science, 2001.
        667-673, 2001.

Dong, J., Shen, C.-C., Kong, X., Wang, H.-C., and Jiang, X.: Reconciliation of hydroclimate
        sequences from the Chinese Loess Plateau and low-latitude East Asian Summer Monsoon

400   regions over the past 14,500 years, Palaeogeography, Palaeoclimatology, Palaeoecology, 435, 127-135, 2015.

Dong, J., Wang, Y., and Cheng, H.: A high-resolution stalagmite record of the Holocene East Asian monsoon from Mt Shennongjia, central China, The Holocene, 20, 257, 2010.

Dorale, J. A., Edwards, R. L., Ito, E., and Gonzalez, L. A.: Climate and vegetation history of the
405   midcontinent from 75 to 25 ka: a speleothem record from Crevice Cave, Missouri, USA, Science, 282, 1871-1874, 1998.

Dorale, J. A. and Liu, Z.: Limitations of Hendy test criteria in judging the paleoclimatic suitability of speleothems and the need for replication, Journal of Cave and Karst Studies, 71, 73-80, 2009.

410   Dykoski, C. A., Edwards, R. L., Cheng, H., Yuan, D., Cai, Y., Zhang, M., Lin, Y., Qing, J., An, Z., and Revenaugh, J.: A high-resolution, absolute-dated Holocene and deglacial Asian monsoon record from Dongge Cave, China, Earth and Planetary Science Letters, 233, 71-86, 2005.

Edwards, R. L., Chen, J., and Wasserburg, G.: ^{238}U-^{234}U-^{230}Th-^{232}Th systematics and the precise measurement of time over the past 500,000 years, Earth and Planetary Science Letters, 81,
415   175-192, 1987.

Fairchild, I., Borsato, A., Tooth, A., Frisia, S., Hawkesworth, C., Huang, Y., McDermott, F., and Spiro, B.: Controls on trace element (Sr-Mg) compositions of carbonate cave waters: implications for speleothem climatic records, Chemical Geology, 166, 255-269, 2000.

Fairchild, I., Smith, C., Baker, A., Fuller, L., Spötl, C., Mattey, D., and McDermott, F.:
420   Modification and preservation of environmental signals in speleothems, Earth Science Reviews, 75, 105-153, 2006.

Fleitmann, D., Cheng, H., Badertscher, S., Edwards, R., Mudelsee, M., Göktürk, O. M., Fankhauser, A., Pickering, R., Raible, C., and Matter, A.: Timing and climatic impact of Greenland interstadials recorded in stalagmites from northern Turkey, Geophysical Research
425   Letters, 36, 2009.

Frisia, S., Fairchild, I. J., Fohlmeister, J., Miorandi, R., Spötl, C., and Borsato, A.: Carbon mass-balance modelling and carbon isotope exchange processes in dynamic caves, Geochimica et Cosmochimica Acta, 75, 380-400, 2011.

Gasse, F.: Hydrological changes in the African tropics since the Last Glacial Maximum,
430   Quaternary Science Reviews, 19, 189-211, 2000.

Genty, D., Baker, A., Massault, M., Proctor, C., Gilmour, M., Pons-Branchu, E., and Hamelin, B.: Dead carbon in stalagmites: carbonate bedrock paleodissolution vs. ageing of soil organic matter. Implications for ^{13}C variations in speleothems, Geochimica et Cosmochimica Acta, 65, 3443-3457, 2001.

435   Genty, D., Blamart, D., Ghaleb, B., Plagnes, V., Causse, C., Bakalowicz, M., Zouari, K., Chkir, N., Hellstrom, J., and Wainer, K.: Timing and dynamics of the last deglaciation from European and North African δ^{13}C stalagmite profiles—comparison with Chinese and South Hemisphere stalagmites, Quaternary Science Reviews, 25, 2118-2142, 2006.

Genty, D., Blamart, D., Ouahdi, R., Gilmour, M., Baker, A., Jouzel, J., and Van-Exter, S.: Precise
440   dating of Dansgaard–Oeschger climate oscillations in western Europe from stalagmite data, Nature, 421, 833, 2003.

Goldsmith, Y., Broecker, W. S., Xu, H., Polissar, P. J., Porat, N., Lan, J., Cheng, P., Zhou, W., and An, Z.: Northward extent of East Asian monsoon covaries with intensity on orbital and millennial timescales, Proceedings of the National Academy of Sciences, 114, 1817-1821,
445   2017.

He, L., Hu, C., Huang, J., Xie, S., and Wang, Y.: Characteristics of large-scale circulation of East Asian monsoon indicated by oxygen isotope of stalagmites, Quaternary Research, 29, 950-956, 2009 (in Chinese with English abstract).

450 Hendy, C. H.: The isotopic geochemistry of speleothems—I. The calculation of the effects of different modes of formation on the isotopic composition of speleothems and their applicability as palaeoclimatic indicators, Geochimica et cosmochimica Acta, 35, 801-824, 1971.

Hu, C., Henderson, G., Huang, J., Xie, S., Sun, Y., and Johnson, K.: Quantification of Holocene Asian monsoon rainfall from spatially separated cave records, Earth and Planetary Science

455 Letters, 266, 221-232, 2008.

Huang, C. C., Pang, J., Zha, X., Su, H., and Jia, Y.: Extraordinary floods related to the climatic event at 4200 a BP on the Qishuihe River, middle reaches of the Yellow River, China, Quaternary Science Reviews, 30, 460-468, 2011.

Huang, C. C., Pang, J., Zha, X., Zhou, Y., Su, H., and Li, Y.: Extraordinary floods of 4100-4000 a

460 BP recorded at the Late Neolithic ruins in the Jinghe River gorges, Middle Reach of the Yellow River, China, Palaeogeography, Palaeoclimatology, Palaeoecology, 289, 1-9, 2010.

Jiang, X., He, Y., Shen, C.-C., Li, Z., and Lin, K.: Replicated stalagmite-inferred centennial-to decadal-scale monsoon precipitation variability in southwest China since the mid Holocene, The Holocene, 23, 841-849, 2013.

465 Jin, G. and Liu, D.: Mid-Holocene climate change in North China, and the effect on cultural development, Chinese Science Bulletin, 47, 408-413, 2002.

Li, T., Shen, C., Li, H., Li, J., Chiang, H., Song, S., Yuan, D., Lin, C., Gao, P., and Zhou, L.: Oxygen and carbon isotopic systematics of aragonite speleothems and water in Furong Cave, Chongqing, China, Geochimica et Cosmochimica Acta, 75, 4140-4156, 2011.

470 Ma, C., Zhu, C., Zheng, C., Wu, C., Guan, Y., Zhao, Z., Huang, L., and Huang, R.: High-resolution geochemistry records of climate changes since late-glacial from Dajiuhu peat in Shennongjia Mountains, Central China, Chinese Science Bulletin, 53, 28-41, 2008.

Maher, B. A.: Holocene variability of the East Asian summer monsoon from Chinese cave records: a re-assessment, The Holocene, 18, 861-866, 2008.

475 McDermott, F.: Palaeo-climate reconstruction from stable isotope variations in speleothems: a review, Quaternary Science Reviews, 23, 901-918, 2004.

Pausata, F. S., Battisti, D. S., Nisancioglu, K. H., and Bitz, C. M.: Chinese stalagmite $\delta^{18}O$ controlled by changes in the Indian monsoon during a simulated Heinrich event, Nature Geoscience, 4, 474-480, 2011.

480 Peng, Y., Xiao, J., Nakamura, T., Liu, B., and Inouchi, Y.: Holocene East Asian monsoonal precipitation pattern revealed by grain-size distribution of core sediments of Daihai Lake in Inner Mongolia of north-central China, Earth and Planetary Science Letters, 233, 467-479, 2005.

Ruan, J., Kherbouche, F., Genty, D., Blamart, D., Cheng, H., Dewilde, F., Hachi, S., Edwards, R.,

485 Régnier, E., and Michelot, J.-L.: Evidence of a prolonged drought ca. 4200 yr BP correlated with prehistoric settlement abandonment from the Gueldaman GLD1 cave, Northern Algeria, Climate of the Past, 12, 1-14, 2016.

Schulz, M. and Mudelsee, M.: REDFIT: estimating red-noise spectra directly from unevenly spaced paleoclimatic time series, Computers & Geosciences, 28, 421-426, 2002.

490 Tan, L., An, Z., Cai, Y., and Long, H.: The hydrological exhibition of 4200 aBP event in China and its global linkages. Geology Review, 54, 94–104, 2008 (in Chinese with English abstract).

Tan, L., Cai, Y., An, Z., Zhang, H., and Qin, S.: Climate patterns in north central China during the last 1800 yr and its possible driving force, Climate of the Past Discussions, 7, 1029-1048, 2011.

495 Tan, L., Cai, Y., Cheng, H., Edwards, L. R., Gao, Y., Xu, H., Zhang, H., and An, Z.: Centennial-to decadal-scale monsoon precipitation variations in the upper Hanjiang River region, China over the past 6650 years, Earth and Planetary Science Letters, 482, 580-590, 2018a.

Tan, L., Shen, C.-C., Cai, Y., Cheng, H., and Edwards, R. L.: Great flood in the middle-lower Yellow River reaches at 4000 a BP inferred from accurately-dated stalagmite records. 500 Elsevier, Science Bulletin, 2018b.

Tan, M. and Cai, B.: Preliminary calibration of stalagmite oxygen isotopes from eastern monsoon China with Northern Hemisphere temperatures, Pages News, 13, 16-17, 2005.

Tan, M.: Circulation background of climate patterns in the past millennium: Uncertainty analysis and re-reconstruction of ENSO-like state, Science China Earth Sciences, 59, 1225-1241, 505 2016.

Tan, M.: Circulation effect: climatic significance of the short term variability of the oxygen isotopes in stalagmites from monsoonal China—dialogue between paleoclimate records and modern cliate research, Quaternary Research, 29, 851-862, 2009 (in Chinese with English abstract).

510 Tan, M.: Circulation effect: response of precipitation $\delta^{18}O$ to the ENSO cycle in monsoon regions of China, Climate Dynamics, 42, 1067-1077, 2014.

Thompson, L. G., Mosley-Thompson, E., Davis, M. E., Henderson, K. A., Brecher, H. H., Zagorodnov, V. S., Mashiotta, T. A., Lin, P.-N., Mikhalenko, V. N., and Hardy, D. R.: Kilimanjaro ice core records: evidence of Holocene climate change in tropical Africa, 515 Science, 298, 589-593, 2002.

Tian, S.-F. and Yasunari, T.: Climatological aspects and mechanism of spring persistent rains over central China, Journal of the Meteorological Society of Japan. Ser. II, 76, 57-71, 1998.

Torrence, C. and Compo, G. P.: A practical guide to wavelet analysis, Bulletin of the American Meteorological Society, 79, 61-78, 1998.

520 Tremaine, D. M., Froelich, P. N., and Wang, Y.: Speleothem calcite farmed in situ: Modern calibration of $\delta^{18}O$ and $\delta^{13}C$ paleoclimate proxies in a continuously-monitored natural cave system, Geochimica et Cosmochimica Acta, 75, 4929-4950, 2011.

Wan, R. and Wu, G.: Mechanism of the spring persistent rains over southeastern China, Science in China Series D: Earth Sciences, 50, 130-144, 2007.

525 Wan, R. and Wu, G.: Temporal and spatial distributions of the spring persistent rains over Southeastern China, Journal of Meteorological Research, 23, 598-608, 2009.

Wan, R., Wang, T., and Wu, G.: Temporal variations of the spring persistent rains and South China Sea sub-high and their correlations to the circulation and precipitation of the East Asian Summer Monsoon, Journal of Meteorological Research, 22, 530-537, 2008.

530 Wang, B. and Lin, H.: Rainy season of the Asian–Pacific summer monsoon, Journal of Climate, 15, 386-398, 2002.

Wang, Y., Cheng, H., Edwards, R., An, Z., Wu, J., Shen, C., and Dorale, J.: A high-resolution absolute-dated late Pleistocene monsoon record from Hulu Cave, China, Science, 294, 2345, 2001.

535 Wang, Y., Cheng, H., Edwards, R., He, Y., Kong, X., An, Z., Wu, J., Kelly, M., Dykoski, C., and Li, X.: The Holocene Asian monsoon: links to solar changes and North Atlantic climate, Science, 308, 854, 2005.

Weiss, H. and Bradley, R. S.: What drives societal collapse?, Science, 291, 609-610, 2001.

Weiss, H., Courty, M.-A., Wetterstrom, W., Guichard, F., Senior, L., Meadow, R., and Curnow, A.:
540   The genesis and collapse of third millennium north Mesopotamian civilization, Science, 261,
       995-1004, 1993.

Wu, L., Zhu, C., Ma, C., Li, F., Meng, H., Liu, H., Li, L., Wang, X., Sun, W., and Song, Y.:
       Mid-Holocene palaeoflood events recorded at the Zhongqiao Neolithic cultural site in the
       Jianghan Plain, middle Yangtze River Valley, China, Quaternary Science Reviews, 173,
545   145-160, 2017.

Xu, H., Hong, Y., Lin, Q., Zhu, Y., Hong, B., and Jiang, H.: Temperature responses to quasi-100-yr
       solar variability during the past 6000 years based on δ^{18}O of peat cellulose in Hongyuan,
       eastern Qinghai–Tibet plateau, China, Palaeogeography, Palaeoclimatology, Palaeoecology,
       230, 155-164, 2006.

550   Yao, F., Ma, C., Zhu, C., Li, J., Chen, G., Tang, L., Huang, M., Jia, T., and Xu, J.: Holocene
       climate change in the western part of Taihu Lake region, East China, Palaeogeography,
       Palaeoclimatology, Palaeoecology, 485, 963-973, 2017.

Yao, T. and Thompson, L. G.: Trends and features of climatic changes in the past 5000 years
       recorded by the Dunde ice core, Annals of Glaciology, 16, 21-24, 1992.

555   Zhang, H., Cai, Y., Tan, L., Cheng, H., Qin, S., An, Z., Edwards, R. L., and Ma, L.: Large
       variations of δ^{13}C values in stalagmites from southeastern China during historical times:
       implications for anthropogenic deforestation, Boreas, 44, 511-525, 2015.

Zhang, H., Cai, Y., Tan, L., Qin, S., and An, Z.: Stable isotope composition alteration produced by
       the aragonite-to-calcite transformation in speleothems and implications for paleoclimate
560   reconstructions, Sedimentary Geology, 309, 1-14, 2014.

Zhang, H., Cheng, H., Spötl, C., Cai, Y., Sinha, A., Tan, L., Yi, L., Yan, H., Kathayat, G., Ning, Y.,
       Li, X., Zhang, F., Zhao, J., and Edwards, R. L.: A 200-year annually laminated stalagmite
       record of precipitation seasonality in southeastern China and its linkages to ENSO and PDO,
       Scientific reports, doi: 10.1038/s41598-018-30112-6, 2018.

565   Zhang, H.: The different precipitation patterns in East Asian monsoon region during Holocene,
       PhD thesis, The University of Chinese Academy of Sciences, 2014 (In Chinese with English
       abstract).

Zhao, L., Ma, C., Leipe, C., Long, T., Liu, K.-b., Lu, H., Tang, L., Zhang, Y., Wagner, M., and
       Tarasov, P. E.: Holocene vegetation dynamics in response to climate change and human
570   activities derived from pollen and charcoal records from southeastern China,
       Palaeogeography, Palaeoclimatology, Palaeoecology, 485, 644-660, 2017.

Zhao, Y., Chen, F., Zhou, A., Yu, Z., and Zhang, K.: Vegetation history, climate change and human
       activities over the last 6200 years on the Liupan Mountains in the southwestern Loess Plateau
       in central China, Palaeogeography, Palaeoclimatology, Palaeoecology, 293, 197-205, 2010.

575   Zhong, W., Cao, J., Xue, J., and Ouyang, J.: A 15,400-year record of climate variation from a
       subalpine lacustrine sedimentary sequence in the western Nanling Mountains in South China,
       Quaternary Research, 84, 246-254, 2015.

Zhong, W., Wei, Z., Chen, Y., Shang, S., Xue, J., Ouyang, J., Cao, J., Chen, B., and Zhu, C.: A
       15.4-ka paleoclimate record inferred from δ^{13}C and δ^{15}N of organic matter in sediments from
580   the sub-alpine Daping Swamp, western Nanling Mountains, South China, Journal of
       Paleolimnology, 57, 127-139, 2017.

Zhong, W., Xue, J., Cao, J., Zheng, Y., Ma, Q., Ouyang, J., Cai, Y., Zeng, Z., and Liu, W.: Bulk
       organic carbon isotopic record of lacustrine sediments in Dahu Swamp, eastern Nanling

Mountains in South China: Implication for catchment environmental and climatic changes in
585   the last 16,000 years, Journal of Asian Earth Sciences, 38, 162-169, 2010a.

Zhong, W., Xue, J., Zheng, Y., Ma, Q., Cai, Y., Ouyang, J., Xu, L., Zhou, S., and Yu, X.: Variations
of monsoonal precipitation over the last 16,000 years in the eastern Nanling Mountains,
South China, Journal of Paleolimnology, 44, 177-188, 2010b.

Zhong, W., Xue, J., Zheng, Y., Ouyang, J., Ma, Q., Cai, Y., and Tang, X.: Climatic changes since
590   the last deglaciation inferred from a lacustrine sedimentary sequence in the eastern Nanling
Mountains, south China, Journal of Quaternary Science, 25, 975-984, 2010c.

Zhou, W., Lu, X., Wu, Z., Deng, L., Jull, A., Donahue, D., and Beck, W.: Peat record reflecting
Holocene climatic change in the Zoigê Plateau and AMS radiocarbon dating, Chinese
Science Bulletin, 47, 66-70, 2002.

595   Zhou, W., Yu, X., Jull, A. T., Burr, G., Xiao, J., Lu, X., and Xian, F.: High-resolution evidence
from southern China of an early Holocene optimum and a mid-Holocene dry event during the
past 18,000 years, Quaternary Research, 62, 39-48, 2004.

Figures and Table
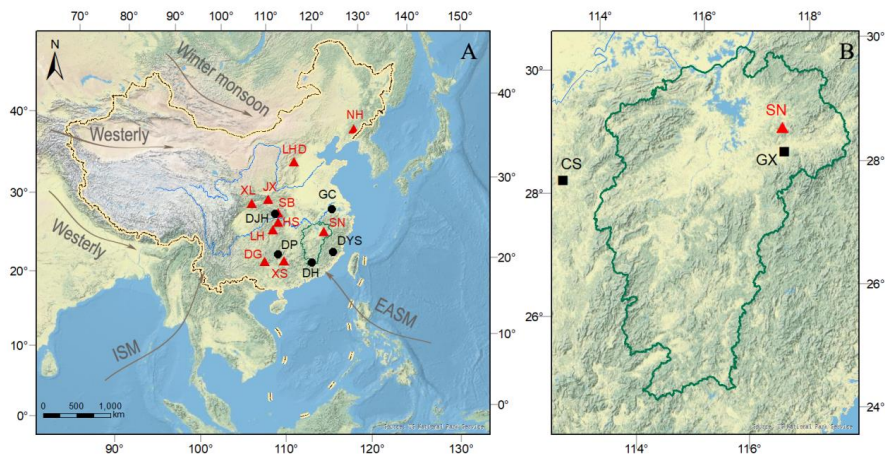
600

Figure 1. Location of Shennong Cave (SN) and other sites mentioned in the paper. Panel A is an overview topographic map and Jiangxi Province is framed by the green line. Black dots indicate the locations of published peat records: GC-Gaochun (Yao et al., 2017), DYS-Daiyunshan (Zhao et al., 2017), DH-Dahu (Zhou et al., 4), DP-Daping (Zhong et al., 2010a) and DJH-Dajiuhu (Ma et

605 al., 2008), and the red triangles show the locations of published stalagmite records: NH-Nuanhe cave (Tan, 2005), LHD-Lianhuadong cave (Dong et al., 2015), JX-Jiuxian cave (Cai et al., 2010), XL-Xianglong cave (Tan et al., 2018), SB-Sanbao cave (Dong et al., 2010), HS-Heshang cave (Hu et al., 2008), LH-Lianhua cave (Zhang et al., 2013), XS-Xiangshui cave (Zhang et al., 2004) and DG-Dongge cave (Wang et al., 2005). Grey arrows denote the directions of East Asian summer

610 monsoon (EASM), Indian summer monsoon (ISM), Westerly and winter monsoon, which affect the climate in China. Panel B is an enlarged map showing the locations of Shennong cave, the Guixi meteorological station (GX) and the GNIP station in Changsha (CS).
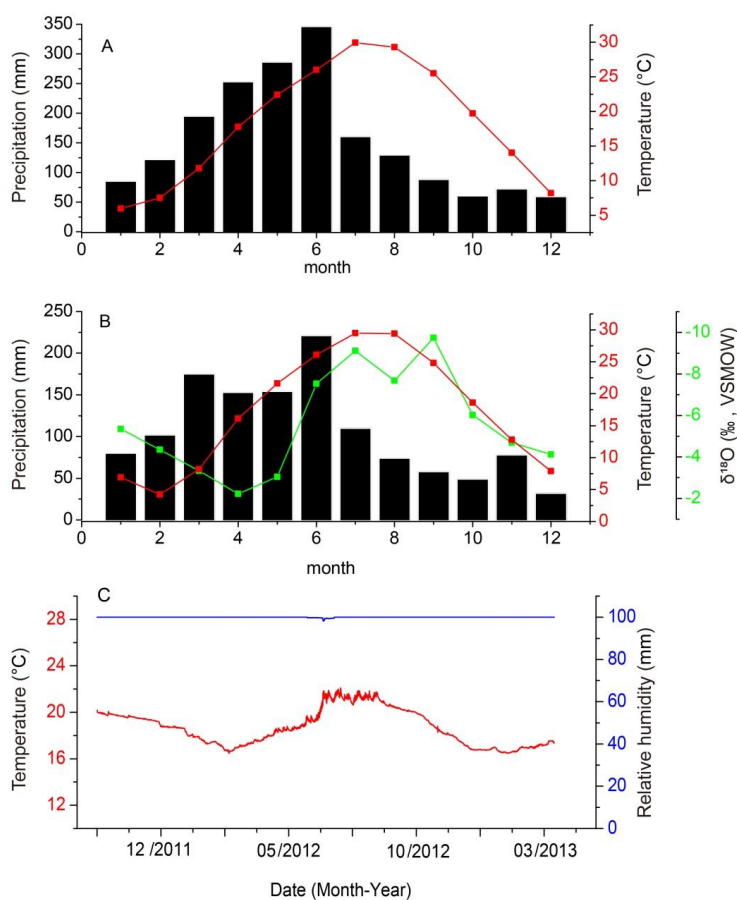
Figure 2. Mean monthly temperature, precipitation and $\delta^{18}O$ value from two meteorological stations close to the study area and environmental monitoring in Shennong cave. (A) Mean monthly air temperature (red line) and precipitation (black column) from the Guixi meteorological station for 1951-2010. (B) Mean monthly air temperature (red line), precipitation (black column) and $\delta^{18}O$ value (green line) from the Changsha GNIP station for 1988-1992. (C) Air temperature (red line) and relative humidity (blue line) in Shennong cave from October 2011 to May 2013.
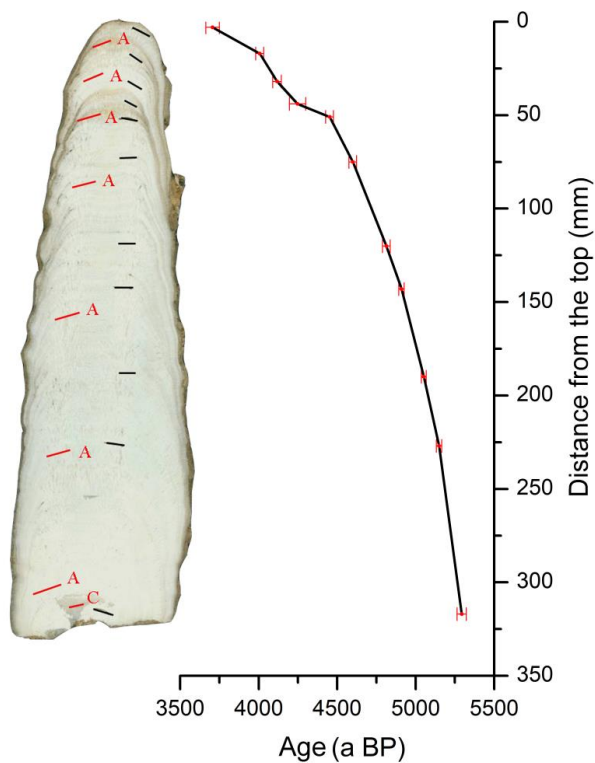
Figure 3. Polished section (left) and age-depth model (right) of stalagmite SN17. Sampling positions for XRD analyses (red lines; A aragonite, C calcite) and ^{230}Th datings (black lines) are

625   shown on the slab. The ^{230}Th dating errors indicated in the right panel are 2σ errors.
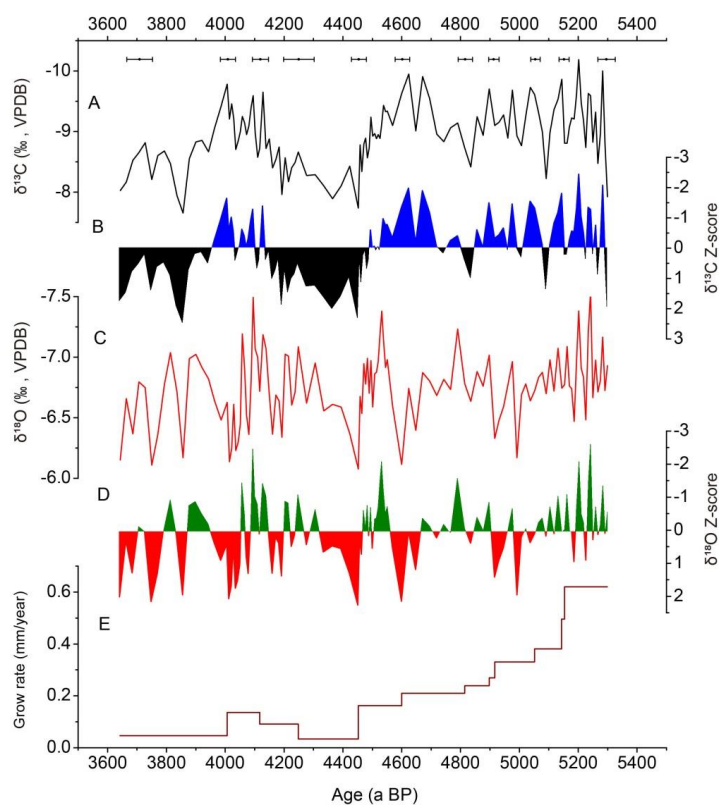
Figure 4. δ¹³C (A) and δ¹⁸O (C) records and growth rate (E) of stalagmite SN17. The δ¹³C and

δ¹⁸O records were normalized to standard records of z-scored δ¹³C (B) and z-scored δ¹⁸O (D) for

630   comparison, respectively. [230]Th dates and error bars are shown on the top of panel A.
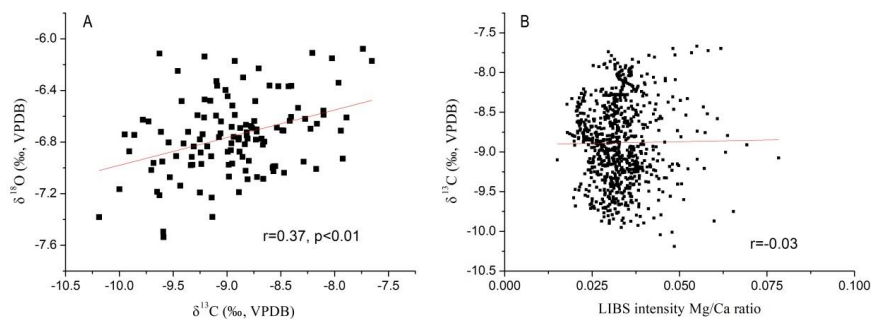
Figure 5. Correlation between δ^{13}C and δ^{18}O values (A) and between δ^{13}C values and Mg/Ca ratios (B) measured along the stalagmite growth axis.

635
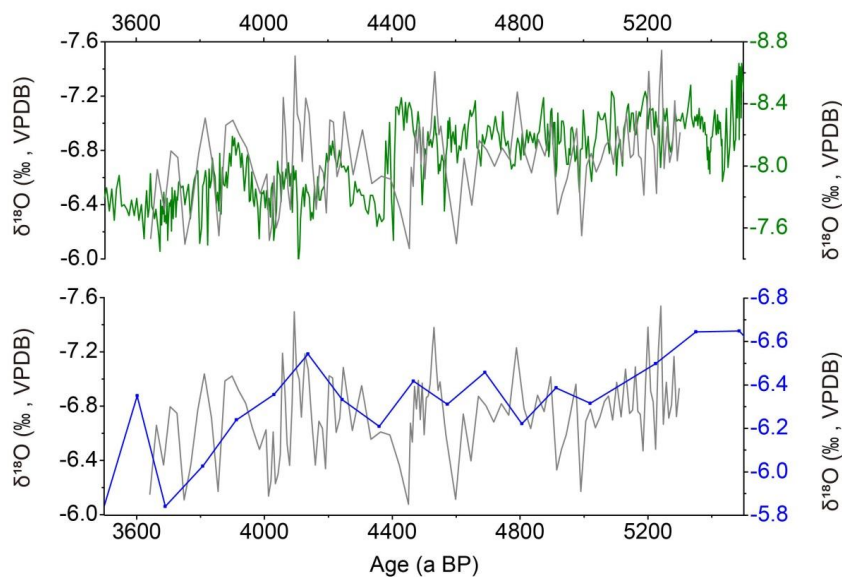
Figure 6. Replication of the δ^{18}O records from Shennong (grey line), Dongge (green line) and Xiangshui (blue line) caves during the overlapping growth period of the three stalagmites.

640
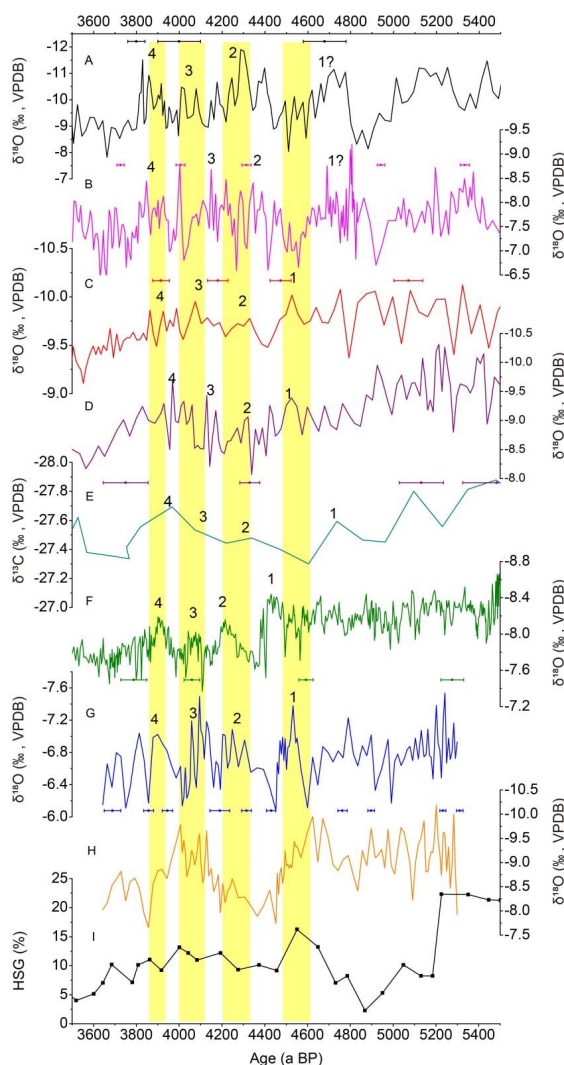
Figure 7. Comparison of δ¹⁸O records from (A) Jiuxian cave (Cai et al., 2010), (B) Xianglong

cave (Tan et al., 2018a), (C) Sanbao cave (Dong et al., 2010), (D) Heshang cave (Hu et al., 2008),

(F) Dongge cave (Wang et al., 2005) and (G) Shennong cave (this study), with δ¹³C records from

645   Dajiuhu peat (E, Ma et al., 2008) and Shennong cave (H, this study), and the ice-rafted

hematite-stained grains (HSG) record from the North Atlantic (Bond et al., 2001). ²³⁰Th dates and

error bars are illustrated with different colors for each stalagmite. The four yellow bars mark four

wet intervals between 4.6 and 3.8 ka BP identified in the δ¹⁸O record of stalagmite SN17

corresponding within error to wet intervals in the other records.

650

Table 1. ^{230}Th results of stalagmite SN17 from Shennong cave. The errors are 2σ.

Sample Number	^{238}U (ppb)	^{232}Th (ppt)	^{230}Th / ^{232}Th (atomic x10^{-6})	d^{234}U* (measured)	^{230}Th / ^{238}U (activity)	^{230}Th Age (yr) (uncorrected)	^{230}Th Age (yr BP)*** (corrected)	d^{234}U$_{Initial}$** (corrected)
SN17-3	1146±1.6	2511±51	320±7	235.3±2.1	0.0426±0.0003	3820±24	3707±43	238±2
SN17-17	2617±5.7	132±10	14960±1115	243.2±2.4	0.0457±0.0003	4076±26	4007±26	246±2
SN17-32	2535±4.9	195±11	10103±565	252.1±2.2	0.0472±0.0003	4187±27	4117±27	255±2
SN17-44	1122±1.2	151±10	6034±420	265.5±1.9	0.0492±0.0006	4319±52	4248±52	269±2
SN17-51	1035±1.7	1169±24	763±16	279.4±1.9	0.0522±0.0002	4540±18	4452±25	283±2
SN17-75	4619±7.3	66±14	61740±12772	268.8±1.9	0.0532±0.0003	4668±25	4600±25	272±2
SN17-120	4640±8.5	225±14	19262±1186	290.3±2.2	0.0566±0.0003	4883±24	4814±24	294±2
SN17-143	2993±5.2	1031±21	2810±58	312.9±2.2	0.0587±0.0002	4980±17	4910±17	317±2
SN17-190	6380±9.5	56±10	114548±20151	322.2±1.4	0.0608±0.0002	5120±16	5052±16	327±1
SN17-227	4436±10.2	873±18	5189±106	323.7±2.2	0.0619±0.0002	5216±17	5149±17	329±2
SN17-317	6886±31.0	2221±45	3273±67	331.7±3.0	0.0640±0.0003	5363±29	5294±29	337±3

U decay constants: λ_{238} = 1.55125×10^{-10} and λ_{234} = 2.82206×10^{-6}. Th decay constant: λ_{230} = 9.1705×10^{-6} (ref. 56). *δ^{234}U = ([^{234}U/^{238}U]$_{activity}$ − 1) ×1000. ** δ^{234}U$_{initial}$ was calculated based on ^{230}Th age (T), i.e., δ^{234}U$_{initial}$ = δ^{234}U$_{measured}$ ×e$^{\lambda234xT}$. Corrected ^{230}Th ages assume the initial ^{230}Th/^{232}Th atomic ratio of 4.4±2.2×10^{-6}. Those are the values for a material at secular equilibrium, with the bulk earth ^{232}Th/^{238}U value of 3.8. The errors are arbitrarily assumed to be 50%.